A Numerical Approach towards Pseudo-Geodesics

Boris Odehnal, Christian Clemenz

University of Applied Arts, Vienna, Austria,
boris.odehnal@uni-ak.ac.at,christian.clemenz@uni-ak.ac.at

Abstract. We compare two different numerical approaches towards pseudo-geodesics on surfaces. On one hand, we solve the system of differential equations numerically using Maple©. On the other hand, we construct pseudo-geodesics on a surface numerically in a discrete setting. The algorithms are tested on torus surfaces, but can easily be applied to any other type of parametrized or discrete surface. We care for sufficient accuracy and stability of the algorithms, not only in order to have optically appealing results, but also in order to be able to derive further geometric properties of pseudo-geodesics, comparable to those known for pseudo-geodesics on cylinders and cones.

Keywords: pseudo-geodesic, numerical construction, approximation

1 Introduction

1.1 Related Work

A curve c_f on a surface $\mathcal{F}$ is called *geodesic* if its principal normals n_c equals the surface normals n_f at each of its point. The curve c_f is called *pseudo-geodesic* if its principal normals enclose a fixed and constant angle φ with the surface normals along the curve. Among the pseudo-geodesics we find the ordinary geodesics ($\varphi = \frac{\pi}{2}$) and the asymptotic lines ($\varphi = 0$). Both types of curves can be found as solutions of a system of ordinary non-linear second order differential equations which allow for exact solutions only in rare and exceptional cases. There do exist some geometric descriptions of geodesics, especially Clairaut's theorem [3] for geodesics on surfaces of revolution. Pseudo-geodesics are given in terms of explicit parametrizations only for cones and cylinders of revolution in [16–18]. In [12], a characterization of the sphere by means of pseudo-geodesics is given and the relations to terminators are disclosed. Numerical approaches towards pseudo-geodesics and meshes built by grids of pseudo-geodesic curves on surfaces are presented in [6, 8]. These approaches aim at optically appealing grids which may find applications in contemporary architecture and design in general. Our aim is a purely geometric one.

1.2 Aims and Methods

While geometric properties of pseudo-geodesics on simple surfaces such as cylinders and cones are described, for more complex surfaces like surfaces of revolution or helical surfaces, no such results are known. Therefore, we hope that a sufficiently accurate numerical approach will give us clues to find parametrizations of pseudo-geodesics on surfaces of revolution. Later, this will allow us to study further geometric properties of pseudo-geodesics.

We will attack this problem by solving the differential equations determining pseudo-geodesic curves numerically (for various initial conditions) in Section 2 and by following pseudo-geodesics on surfaces from initial conditions along with the geometric condition that the angle φ between the curve's normal and the surface normal (or equivalently, the curve's osculating plane and the surface's tangent plane) remains constant over the course of the curve in Section 3. Both approaches will be tested on torus surfaces, for they are on one hand sufficiently complex, *i.e.*, they are of genus 1, they show regions of positive and negative Gaussian curvature, and they have either 2, 1, or 0 singular points. On the other hand, these surfaces are sufficiently simple: They are closed surfaces of revolution and carry four independent one-parameter families of circles. The latter two properties may increase the chance of finding closed or periodic pseudo-geodesics. The rather short Section 4 summarizes observations while repeatedly and numerically/geometrically integrating the differential equations of the pseudo-geodesics. From a numerically determined plot in the parameter domain, we may be able to guess or fit best approximating closed parameter curves or approximate the plot by means of Fourier series. This will briefly be sketched in Section 5 and may at least lead to approximate parametrizations of pseudo-geodesics, or in the best case, it may lead to a closed form representation of pseudo-geodesics on the underlying surface. We admit that some of the constructions and computations may fit perfectly well for the torus, since this is the surface we use most of the time. Whenever there is a difference to the case of an arbitrary base surface, we shall explicitly say so.

2 Numerical Solution of the Differential Equations

2.1 Differential Geometric Preparations

In the first numeric approach, we shall look for numeric solutions of the differential equations of pseudo-geodesics on a surface. Therefore, we shall briefly describe how to write down these equations. A derivation of them can be found in [12] and a more detailed description of the elementary differential geometry of curves and surfaces can be found in [3, 7, 13, 14].

Let $f : U \subset \mathbb{R}^2 \to \mathbb{R}^3$ be a C^2 parametrization of a surface $\mathcal{F} = f(U)$ in Euclidean three-space with only regular points in U. Let further $c(t) = (u^1(t), u^2(t)) : I \subset U \to \mathbb{R}^2$ be a curve in the parameter domain U, then $c_f := f \circ c = (f^i(u^1(t), u^2(t)))$ is a surface curve on $f(U)$. Then, $\mathrm{I} = g_{ij}\mathrm{d}u^j\mathrm{d}u^j$

denotes the first fundamental form of f and $g_{ij} = \langle \partial_i f, \partial_j f \rangle$ (with $\langle x, y \rangle$ denoting the canonical inner product of two vectors x, y). The Christoffel symbols of the first kind are $\Gamma_{ijk} = \frac{1}{2}(-\partial_k g_{ij} + \partial_j g_{ki} + \partial_i g_{jk})$ and determine those of the second kind according to $\Gamma_{ij}^k = \Gamma_{ijl} g^{lk}$, where $(g^{ij}) = (g_{ij})^{-1}$. Here, and in what follows, the Einstein convention on sums is used: An index that appears as superscript and subscript at the same time serves as a summation index. The curvature analysis of surfaces needs the unit normal vector field $n_f : U \subset \mathbb{R}^2 \to \mathrm{S}^2$, which, based on the parametrization, is obtained by $n_f := \partial_1 f \times \partial_2 f / \sqrt{G}$, where $G := \det(g_{ij})$ (with $\times$ denoting the exterior product induced by the canonical scalar product). Then, the second fundamental form of f reads $\mathrm{II} = h_{ij} \mathrm{du}^i \mathrm{du}^j$, where $h_{ij} = \langle n_f, \partial_i \partial_j f \rangle$. If now $-\frac{\pi}{2} < \varphi < \frac{\pi}{2}$ denotes the angle enclosed by the curve's principal normal n_c and the surface normals n_f along the curve, then, according to [12], the differential equations of the pseudo-geodesics are

$$\ddot{c}^l + \Gamma_{ij}^l \dot{c}^i \dot{c}^j - \cot\varphi \, h_{ij} \varepsilon_{rs} g^{sl} \dot{c}^r \dot{c}^i \dot{c}^j = 0, \quad l = 1, 2, \tag{1}$$

where a dot indicates derivatives with respect to the arc-length parameter and ε_{ij} are the components of the skew-symmetric ε-tensor with $\varepsilon_{12} = 1$.

For initial data consisting of a point $P_0 = (u_0^1, u_0^2) \in U$ and an initial tangent (unit) vector $v_0 = (\mathrm{du}_0^1, \mathrm{du}_0^2)$, there exists a solution of (1), at least locally. These solutions are the pseudo-geodesics on $f(U) = \mathcal{F}$. Among them, we find the ordinary geodesics corresponding to $\varphi = \pm\frac{\pi}{2}$ and the asymptotic curves corresponding to $\varphi = 0$.[1] We shall exclude the ordinary geodesics and the asymptotic curves from our considerations, the latter because they do only exist in regions of negative Gaussian curvature.

For the case of a torus, we shall not forget that meridian circles are pseudo-geodesics, since meridians are geodesics on surfaces of revolution in any case. The parallel circles form another class of pseudo-geodesics, while they are not ordinary geodesics. Their osculating plane is constant, whence their principal normal is also constant and encloses a constant angle with the surface normal along the parallel circle. Explicit solutions of the equation of ordinary geodesics on the torus are known (cf. [4, 10]) and shall, therefore, not be discussed here. It is not so easily verified that none of the curves given in [4, 10, 19] can be found among the pseudo-geodesics.

Figure 1 shows some examples of apparently closed pseudo-geodesics obtained as numerical solutions of (1). These are the hopeful candidates when it comes to curve fitting. Moreover, among the closed curves we may also find algebraic pseudo-geodesics on the torus if they do exist.

2.2 Numerical Determination of Pseudo-Geodesics with Maple©

The numerical solutions of (1) could be derived with any computer algebra system that allows for the numerical solution of systems of ordinary differential equations. For our own convenience, we have chosen Maple©.

[1] In order to capture the limit cases of asymptotic curves and ordinary geodesics, one ought to replace the cotangent by $\cos\varphi / \sin\varphi$, and subsequently multiply the differential equation (1) by $\sin\varphi$.

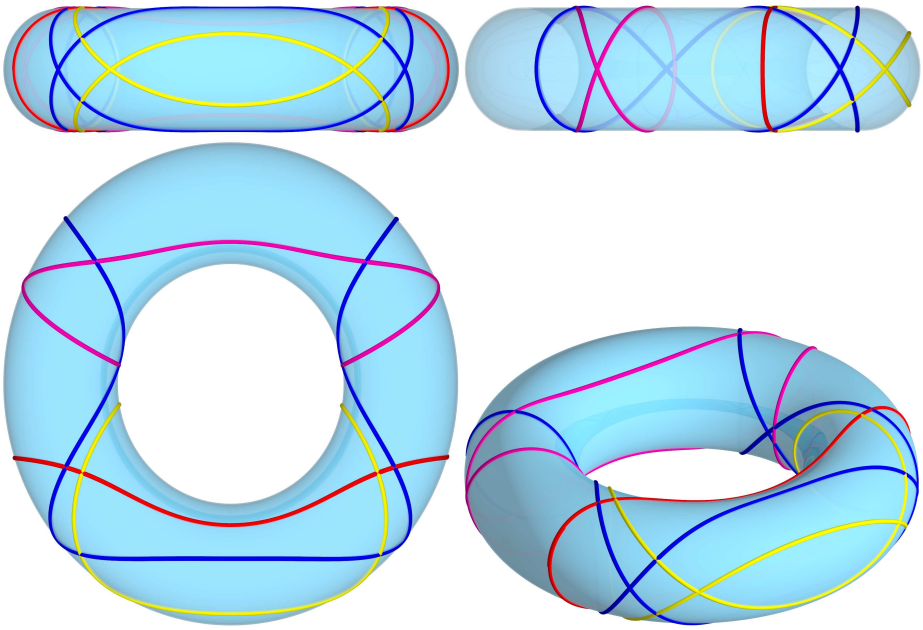

Fig. 1. Some closed pseudo-geodesics on a ring torus: front view and side view (top), top view and axonometric image (bottom).

It is favorable to use Maple©'s built-in function

$$\texttt{dsolve}(\{\texttt{odes}, \textit{initial\_values}\}, \{u^1(\texttt{t}), u^2(\texttt{t})\}, \texttt{numeric},$$
$$\texttt{method} = \textit{Method}, \texttt{relerr} = e_{\text{rel}}, \texttt{abserr} = e_{\text{abs}}, \texttt{output} = \texttt{procedurelist});$$

where `odes` are the ordinary differential equations (1) prepared in a separate procedure, `initial_values` are the initial values $P_0 = (u_0^1, u_0^2)$ (starting point) and $v_0 = (\dot{u}_0^1, \dot{u}_0^2)$ (tangent unit vector P_0). We shall restrict the search of pseudo-geodesics by setting $u_0^2 = 0$. This means no loss of generality, since the property of being pseudo-geodesic is invariant under rotations about the torus's axis. The coordinate u_0^1 is allowed to trace the entire unit circle. This is also the case for the tip of v_0. The option *Method* can either be `rkf45`, `kf45_dae` or `ck45`, `ck45_dae` which are mainly Runge-Kutta methods (fourth and fifth order, Fehlberg method) or Runge-Kutta methods with Cash-Karp coefficients. Further, Maple© renders Rosenbrock methods (option `rosenbrock`) and higher order Runge-Kutta methods (option `dverk78`) among others. For details on numerical methods for ODEs, we refer to [1, 2, 15]. All these methods were used and compared in order to show that for sufficient tolerances $e_{\text{rel}} < 10^{-6}$ and $e_{\text{abs}} < 10^{-8}$ the difference between the various results can hardly be seen (measured in thousands of the principal radius of the torus). The output yields a list of points $P_i = (u_i^1, u_i^2)$ forming a discrete curve in the parameter domain that can be raised via the surface parametrization onto the surface. The results are

then exported into a POV-Ray [9] include file and rendered. Some numerical solutions of (1) displayed in Fig. 1. These curves seem to be closed.

Of course, we get some discrete curve in that way. However, it is only a numerical solution of (1), we still have to check the quality of the solution by calculating the angles $\varphi_i = \sphericalangle(n_{ci}, n_f(P_i))$ and checking whether they are equal to the initially chosen value φ up to a certain tolerance. Figure 2 shows the plot of the angle φ for a numerical solution. After approximately 4400 points the curve

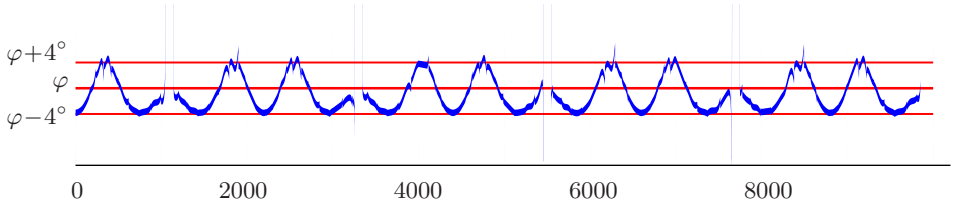

Fig. 2. Diagram of the angle φ enclosed by the normals of $\mathcal{F}$ and the principal normals of the blue pseudo-geodesic from Fig. 1.

is almost closed. The angle graph in Fig. 2 shows that even twice the amount of points does not really increase the inaccuracies. Unfortunately, we observe some jumps. The rather big deviations of the angles φ_i from φ motivate the second approach, *i.e.*, the constructive numerical approach towards pseudo-geodesics.

3 Numerical Construction of Pseudo-Geodesics

3.1 Some Constructive Differential Geoemtry

The assumptions on the underlying surface $\mathcal{F}$ are those made in Section 2. Now, the surface is given as a triangle mesh. At each point P on the surface, a unique unit normal n_f is either given or can be computed from the triangulated surface. In the case of a torus, the normal (line) meets the spine curve (trace of centers of all meridians) and the torus's axis, too (cf. Fig. 4, right).

The initial condition consists of the point P_0, a (not necessarily normalized) tangent vector $v_0 = (\mathrm{d}u^1, \mathrm{d}u^2)$, and the constant angle φ enclosed by the surface normal n_f and the curve's principal normal n_c. The distribution of normal curvatures at P_0 is described by the Dupin indicatrix (see [5, 13, 14]) and is computed via the first and second fundamental form as $\kappa_n(v_0) = \mathrm{II}(v_0)/\mathrm{I}(v_0)$.

In the case of a torus with parametrization

$$f(u^1, u^2) = \big((R + r\cos u^1)\cos u^2, (R + r\cos u^1)\sin u^2, r\sin u^1\big)$$

with $(u^1, u^2) \in [0, 2\pi[^2$ and $r, R \in \mathbb{R} \setminus \{0\}$, the principal curvatures can be easily determined and read $\kappa_1 = \cos u^1/(R + r\cos u^1)$ and $\kappa_2 = 1/r$.

According to Euler's formula (cf. [5, 14]),

$$\kappa_n = \kappa_1^2 \cos\alpha + \kappa_2^2 \sin\alpha, \tag{2}$$

where κ_1, κ_2 are the $\mathcal{F}$'s principal curvatures at P_0 and α_0 is the angle enclosed by the first principal tangent and the curve's tangent (vector v_0) at P_0. Further,

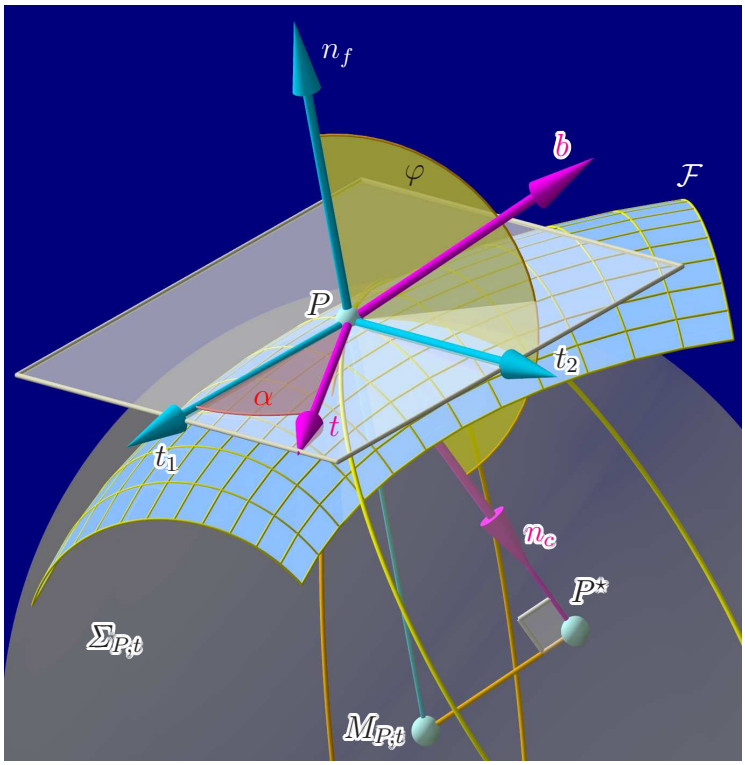

Fig. 3. At any point P of a curve c_f (the curve is not shown) in a surface $\mathcal{F}$ and for any (non-asymptotic) tangent t at P, the osculating circles of all curves through P tangent to t lie on the Meusnier sphere $\Sigma_{P,t}$. (The unnecessary index $_0$ is suppressed.)

we make use of MEUSNIER's theorem: The osculating circles of all surface curves on $\mathcal{F}$ through P with tangent direction v form a sphere (cf. [5, 14]), the Meusnier sphere Σ_{P_0,v_0} whose center is a point on n_f at P_0 at distance $\rho_n = \frac{1}{\kappa_n}$ from P_0, see Fig. 4 (2). Therefore, the curvature radius ρ_c of c_f at P_0 is equal to

$$\rho_c = \rho_n \cos\varphi. \tag{3}$$

Figure 3 illustrates the relations between the osculating circles of the normal section and some section through a given surface tangent.

3.2 The Numeric Construction

The numerical construction of the curve consists of the following steps:
(i) Choose an initial point $P_0 \in \mathcal{F}$, a tangent unit vector v_0 enclosing some angle

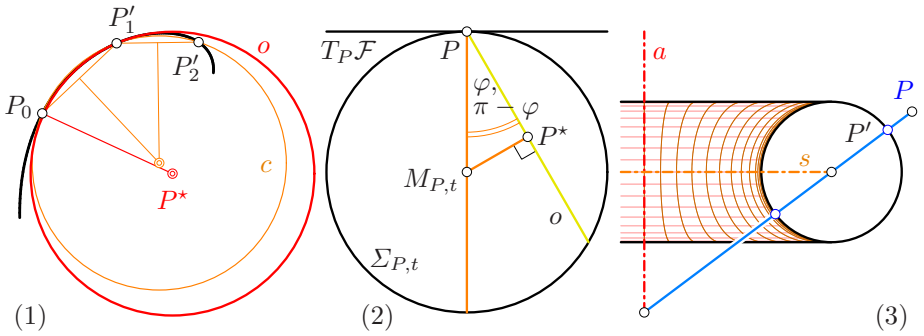

Fig. 4. (1) Approximation of the osculating circle o by the circumcircle c of close points. (2) The Meusnier $\Sigma_{P,t}$ sphere carries the osculating circles of all surface curves touching t at P. (3) The point P' closest to P on a torus surface $\mathcal{F}$ is the orthogonal projection of P onto $\mathcal{F}$. Any normal of $\mathcal{F}$ meets the axis a and the spine circle s.

α_0 with the first principal curvature tangent (*i.e.*, the tangent to the meridian circle through P_0). Note that this angle will change during the course of the pseudo-geodesic.
(ii) Determine the surface normal n_f at P_0 and the curvature radius $\rho_n(v_0)$ of the normal sections through v_0. Then, use (3) in order to determine the radius $\rho_c(\varphi)$ of the desired pseudo-geodesic's osculating circle o_0 at P_0. The plane of the osculating circle o_0 encloses the initially chosen and fixed angle φ with $\mathcal{F}$'s tangent plane $T_{P_0}f$.
(iii) The osculating circle o_0 of the pseudo-geodesic starting at P_0 in the direction v_0 is used as approximation of the pseudo-geodesic branch c_f. Depending on the local curvature (or equivalently, the size of the osculating circle), we fix a certain step size to march twice forward and find two points P_1' and P_2' (which do, in general, not lie on $\mathcal{F}$). This yields a new point P_1 on c_f after projecting the point P_1' on the circle onto the surface. P_1' is always the closest to P_1. The projection of P_2' on $\mathcal{F}$ is the point P_2 and the tangent to c_f at the new point P_1 is parallel to the line $[P_0, P_2]$.
(iv) Then, restart at (i) with $P_0 = P_1$ and v_0 equals the normalized vector $P_2 - P_0$. The course angle α_0 changes and is to be determined anew, for it equals the angle between the first principal curvature tangent (tangent to the meridian) and the new tangent vector $P_2 - P_0$. Especially for the torus, we determine the local coordinates (u_i^1, u_i^2) for a point P_i in order to make use of (2) and (3) and in order to describe the curve in the parameter domain (for later approximation).

We shall not hide that the numerical construction exhibits some problems:
(1) The course angle α (between the tangent of the curve and the meridian circles' tangents) will change. Therefore, in hyperbolic regions of the surface, the curve tangent may eventually become an asymptotic tangent. Then, the pseudo-geodesic has an inflection point and the approximation of the pseudo-geodesic's tangent by means of the chord joining neighbouring points on the osculating circle will fail. In these cases, the asymptotic tangent at P_0 replaces the osculating

circle and the step size is chosen very small compared to the step size on the last regular osculating circle before.
(2) The curvature of the numerically integrated pseudo-geodesic curve may become arbitrarily large (especially in the vicinity of singular points as may occur on spindle and thorn tori). Then, the osculating circle becomes rather small and the approximation of the tangents may become highly inaccurate. Thus, the step size on the circle has to be chosen very carefully.

In the case of a torus, some of the construction steps are simplified. This means especially the construction of surface normals and the orthogonal projection onto the surface (which works as described above). Further, for the torus, it is rather simple to reconstruct the local coordinates (u^1, u^2) of a newly constructed point on the surface. Therefore, we do not have to approximate normal curvatures and curvature of arbitrary surface curves by means of locally approximating paraboloids (or other auxiliary surfaces) and can use (2) and (3) in order to find curvature radii. This increases the accuracy of the algorithm and accelerates it.

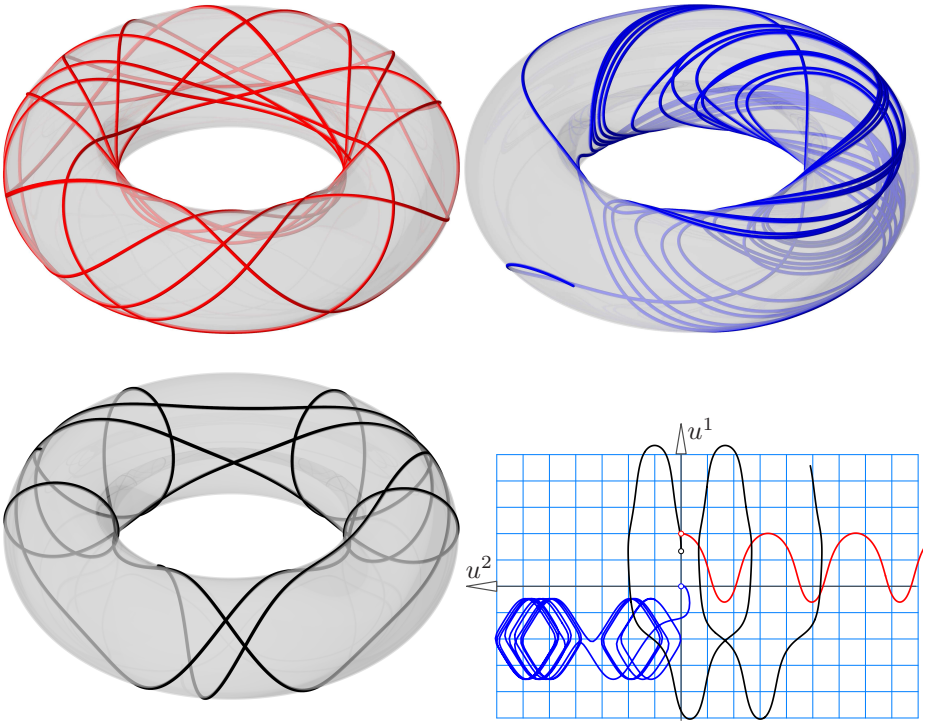

Fig. 5. Some open pseudo-geodesics and the corresponding curves in the parameter domain (bottom, right).

4 The Questionable Cases: Open Curves

It is yet unclear whether pseudo-geodesics are open because of a special choice of the initial conditions or numerical inaccuracies. However, since geodesics on surfaces and especially on tori (and other surfaces of revolution) are open in the vast majority of cases (initial conditions), we can expect that pseudo-geodesics show the same behaviour. Figure 5 shows three examples of pseudo-geodesics that do not close (at least in the interval under consideration). Most likely, they will not close regardless of how long we continue the numerical integration.

While the red and the black curve in Fig. 5 are open and correspond to periodic curves in the parameter domain, the blue curve seems to wind around the torus after it has left the initial point in the opposite direction of the region where it oscillates.

5 Approximation of the Curves in the Parameter Domain

The closed pseudo-geodesic curves on the torus either correspond to closed curves in the parameter domain or to periodic curves (with period length 2π), see Fig. 6. Open, oscillating, or meandering curves may also correspond to periodic curves in the parameter domain (but with period length different from 2π) or seem to converge towards some limit shape which is not necessarily an attractor as can be seen in Fig. 5.

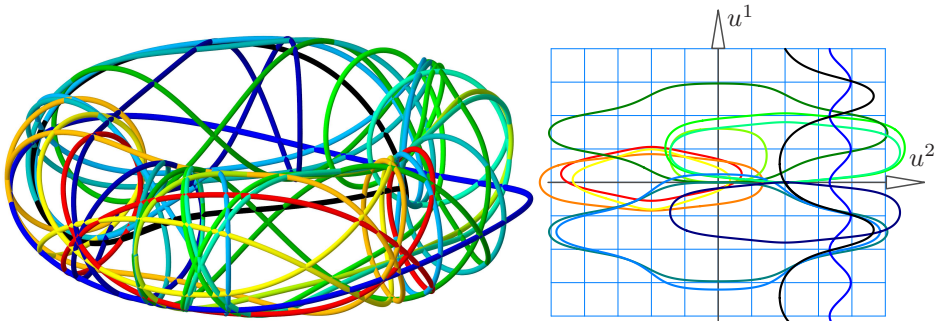

Fig. 6. Some apparently closed pseudo-geodesics (left) and the corresponding curves in the parameter-domain (right).

Both kinds of curves can be approximated by means of Fourier series: Each entry from the list of (u^1, u^2) coordinates can be interpreted as a (discrete) coordinate function $u^1(t)$ and $u^2(t)$ of the pseudo-geodesic curve over time or the counter of the iteration step t. As such, Fourier series can be used to approximate these individual functions, given a sufficient amount of variable parameters. We used the least squares optimization of the symfit library [11] to adjusts these parameters in order to fit best-approximating curves to $u^1(t)$ and $u^2(t)$. The

resulting curves are then combined again to get first the curves in the parameter domain, and then, an approximation of the pseudo-geodesic curve on the surface. Two specific examples are shown in Figure 7. Provided that the Fourier series are expanded in sufficiently many terms, and further, that the coefficients show a specific behavior, one may guess a simpler, eventually closed form representation of the curves. Such a parametrization may give further insight on potential curve patterns via the parameter values of the Fourier series.

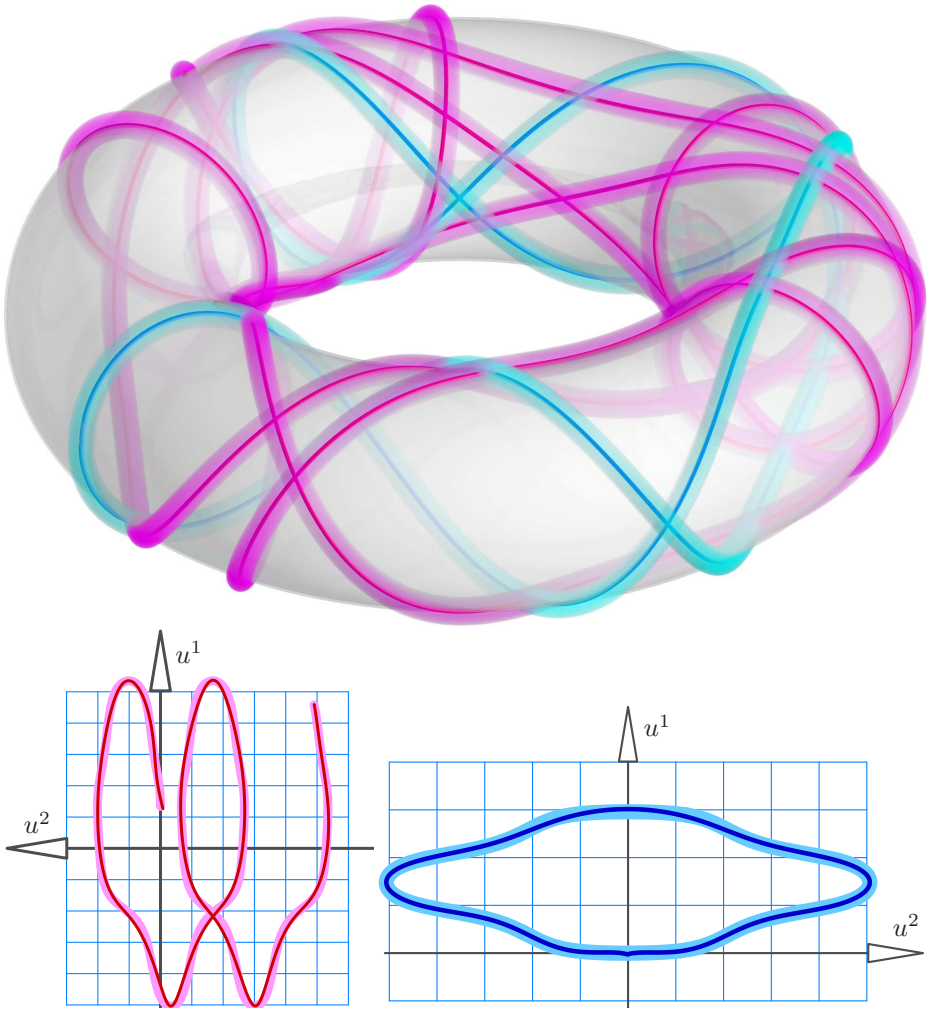

Fig. 7. Top: Comparison of numerically determined pseudo-geodesics (hollow, thick) with their best-approximations (thin). Bottom: Best approximation of the (u^1, u^2)-plot by means of Fourier series expansion for an open (red) a closed (blue) curve. The hollow tubes are the curves to be approximated.

6 Conclusion and Future Work

We have observed that there do exist open and closed pseudo-geodesics and that the two numerical approaches do produce similar results. Thus, they are most likely of the same quality and are well suited for the numerical construction of pseudo-geodesic curves. The numerical constructive approach is to be preferred, since the geometric condition on the curve (constant angle φ) is satisfied anyhow.

As seen from the numerical results, pseudo-geodesics can be divided into the following groups:
(a) open,
(b) closed (sometimes contractible to a point) or
(c) wrapped around the torus (topologically, some knot different from a circle),
(d) stay within a torus region bounded by two parallel circles (topologically equivalent to a circle).

The numerical derivation of further properties, such as special shapes and behaviour of the tangent surface of pseudo-geodesics is still to be done. However, due to the highly accurate numerical results, these derivations are near and seem to deliver promising results.

The numerical results and the approximations of curves in the parameter domain needs further inspection. It is not yet clear whether we can find simple closed form parametrizations of pseudo-geodesic curves.

References

1. Butcher J.C.: *The numerical analysis of ordinary differential equations: Runge-Kutta and general linear methods.* John Wiley & Sons, Chichester, New York, 1987.
2. Cash J.R., Karp A.H.: *A variable order Runge-Kutta method for initial value problems with rapidly varying right-hand sides.* ACM Transactions on Mathematical Software **16** (1990), 201–222.
3. Do Carmo M.P.: *Differential Geometry of Curves and Surfaces.* Prentice Hall, 1976.
4. Kerner M.: *Geschlossene geodätische Linien auf einem Kreistorus.* Mh. Math. Phys. **38** (1931), 53–56.
5. Kruppa E.: *Analytische und Konstruktive Differentialgeometrie.* Springer-Verlag, Wien, 1957.
6. Mesnil R., Baverel O.: *Pseudo-geodesic grid shell.* Engineering Structures **279** (2023), pp. 115558.
7. Oprea J.: *Differential Geometry and Its Applications.* 2nd edition, Prentice Hall, NJ, 2004.
8. Pham-Trong V., Szafran N., Biard L.: *Pseudo-geodesics on three-dimensional surfaces and pseudo-geodesic meshes.* Numer. Algorithms **26**/4 (2001), 305–315.
9. POVRay: *The persistence of vison ray tracer.*
   Available at: `https://github.com/POV-Ray/povray`
10. Puchta A.: *Loxodromen und kürzeste Linien auf dem Kreisring.* Mh. Math. Phys. **1** (1890), 443–450.
11. Roelfs M., Kroon P.C.: *tBuLi/symfit: symfit 0.5.6.* Zenodo, Feb. 15, 2023. doi: 10.5281/zenodo.7643591.

12. Simon U.: *Pseudogeodätische Linien auf Flächen.* Acta Math. Acad. Sci. Hunga. **22** (3–4) (1972), 325–330.
13. Spivak M.J.: *A Comprehensive Introduction to Differential Geometry.* Publish or Perish, 1999.
14. Strubecker K.: *Differentialgeometrie.* Vol. III, Theorie der Flächenkrümmung. Sammlung Göschen Band 1180/1180a, W. de Gruyter & Co., Berlin, 1969.
15. Wanner G., Hairer E.: *Solving ordinary differential equations II.* Vol. 375, Springer Berlin-Heidelberg-New York, 1996.
16. Wunderlich W.: *Pseudogeodätische Linien auf Zylinderflächen.* Sitz. Ber. Akad. Wiss. Wien **158** (1–5) (1950), 61–73.
17. Wunderlich W.: *Pseudogeodätische Linien auf Kegelflächen.* Sitz. Ber. Akad. Wiss. Wien **158** (1–5) (1950), 75–105.
18. Wunderlich W.: *Raumkurven, die pseudogeodätische Linien eines Zylinders und eines Kegels sind.* Comp. Math. **8** (1951), 169–184.
19. Wunderlich W.: *Über die Torusloxodromen.* Mh. Math. Phys. **56** (1952), 313–334.